Improved hetero-junction interface through Cation alloying for Wide-gap Pure-sulfide Cu(In,Ga)S_2: Pathway to Over 1 V Open-circuit Voltage

Guojun He[1], Kaiwen Sun[1], Chang Yan[2], Shujie Zhou[3], Xiaojie Yuan[1] and Xiaojing Hao[1]

[1]*Australian Centre for Advanced Photovoltaics, School of Photovoltaic and Renewable Energy Engineering, University of New South Wales, Sydney, NSW 2052, Australia*
[2]*Sustainable Energy and environment Thrust, The Hong Kong University of Science and Technology (Guangzhou), Guangzhou, 511400, China*
[3]*School of Chemical Engineering, University of New South Wales, Sydney, NSW 2052, Australia*
xj.hao@unsw.edu.au

Introduction

The current power conversion efficiency (PCE) of commercialized Si solar cells is approaching its theoretical limits, as defined by the detailed balance theory.[1, 2]To overcome this limitation and convert more green sunlight energy into electricity, tandem solar cell has emerged as the most promising technology for the future. Among different tandem solar cell options, Si-based tandem with wide bandgap (E_g) material for top cells are the most popular tandem solar cell concept. However, the lack of suitable wide-gap top cell is currently obstructing the technology from advancing. Pure-sulfide chalcopyrite Cu(In,Ga)S_2 (CIGS) is one of the most promising options for top cell, as it has high efficiency potential, ecofriendly constitutions, low-cost as well as stable nature.[3]

Although low-E_g chalcopyrite Cu(In,Ga)Se_2 has achieved a record efficiency of 23.60 %[4], the efficiency of pure-sulfide CIGS has stagnated at 15.50 % since 2016.[5] The performance of CIGS is mainly hindered by large open circuit voltage (V_{OC}) deficit (E_g /q - V_{OC}), which can mainly be attributed to recombination loss at the interface and bulk. For CIGSe solar cells, CdS buffer layer can achieve a desirable spike-like band alignment at p-n interface, contributing to a high-quality junction. Compared to low bandgap CIGSe, high bandgap CIGS with a higher conduction band minimum (CBM) suffers from an unfavoured cliff-like configuration with CdS which results in severe interface recombination.[6] Besides, the performance CIGS is also limited by abundant bulk recombination via higher deep defect density and thus a much shorter minority carrier lifetime than that of CIGSe when substitute Se with S.[7] Hence, the passivation of the interface and bulk recombination would be the key to reduce V_{OC} deficit and make CIGS more competitive for top cell candidate for tandem solar cells.

In this study, we developed a cation-alloying technique for wide bandgap pure-sulfide CIGS. We sputtered a thin Ag bottom layer followed by CuGa-CuIn co-sputtering, and then sulfurized the sample in rapid-thermal processer with sulfur pellets at high temperature. The rest of the process was the same as we described in our previous paper.[3] We achieved a power conversion efficiency of 12.24 % device with 16.0 % Ag-alloying (Defined as Ag/(Ag+Cu) atomic ratio) without anti-reflection coatings (ARC) with a significantly improved interface quality. The improvement may be attributed to minimized CBO and improved J_{02} characterized by Suns-V_{OC}.

Results and discussions

The critical crystallinity and grain growth were examined by SEM and XRD. Unlike many have been reported before, Ag-alloying did not result in better crystallinity and grain growth, except the 20.0 % Ag-alloying sample. This 20 % Ag-alloying presents better crystallinity alongside with larger grains, as shown in Figure 1(e). However, SEM alone is insufficient to define the crystallinity and grain growth as it only shows a certain area of the samples. XRD may provide a better understanding on crystallinity and grain growth. The XRD results shown in Figure 2 are well agreed with the SEM images: first of all, Ag has successfully incorporated into the CIGS bulk, as the peak shifted to lower angel due to the larger Ag atom size with Ag substitution on Cu sites, which means the effects can be attributed to Ag-alloying; secondly, the intensity of the major CIGS peak did not improve; furthermore, the full width at half maximum (FWHM) did not shrink as the Ag incorporated. Combining SEM and XRD, we can conclude that Ag-alloying may not be the key to affect the crystallinity and grain growth.

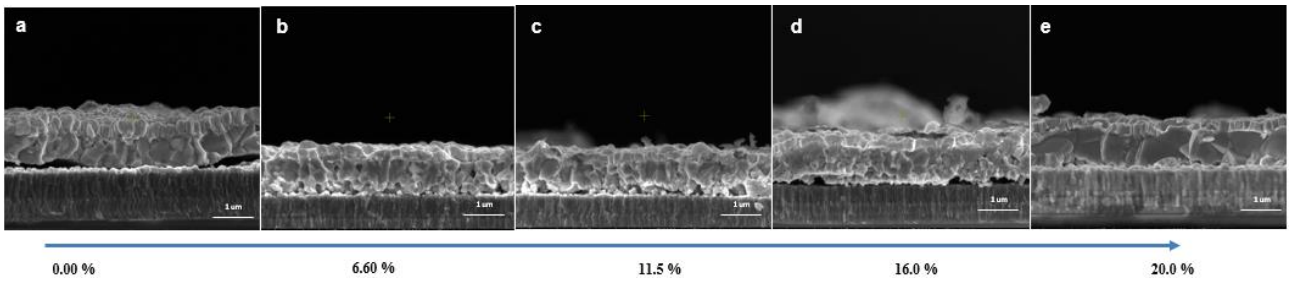

Figure 1. Cross-sectional SEM with corresponding Ag-alloyed percentage

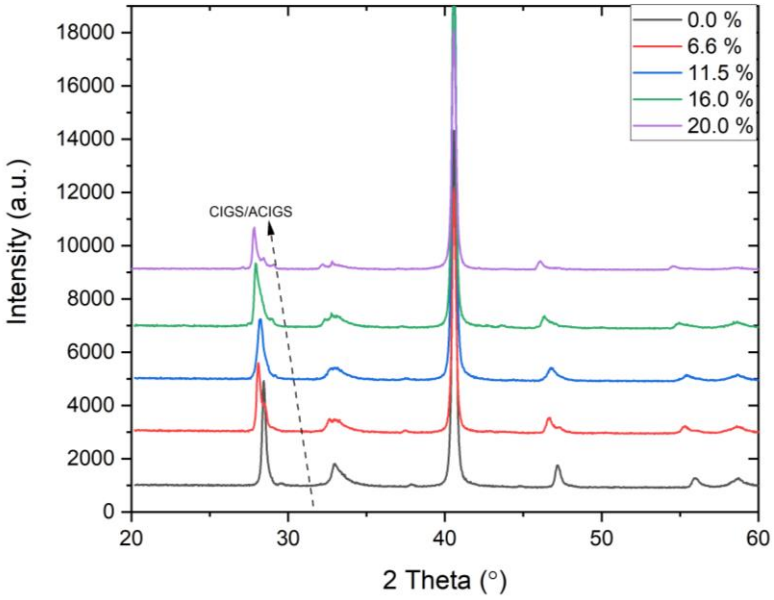

Figure 2. XRD results of different Ag (%)-alloyed CIGS

Table 1 presents the device performance of different Ag(%)-alloying CIGS, showing the achieved highest efficiencies. The sample with 16.0 % Ag-alloying exhibited a peak efficiency gain of 3.65 % compared to the sample without Ag-alloying. More importantly, Ag-alloying significantly reduces the V_{OC} deficit from 792 mV to 702 mV, resulting in a significant improvement on ~ 100 mV V_{OC} gains. Additionally, Ag-alloying led to a significant improvement on fill factor (FF), with the performance of FF rising to ~ 67 % and to over 70 %, when compared to the sample without Ag-alloying.

Table 1 Device Performance

Sample	Jsc (mA/cm^2)	Voc (mV)	FF (%)	Eff (%)	Eg (eV)	Voc Deficit (mV)
0 %	17.50	777.22	63.13	8.59	1.57	792.78
11.5 %	18.69	838.90	70.65	11.08	1.57	731.1
16.0 %	19.70	887.97	69.98	12.24	1.59	702.03
20.0 %	17.50	860.41	66.90	10.08	1.59	729.59

Table 2 Characterization results by Suns - V_{OC}

Sample	Voc (mV)	p.FF	Ideality Factor	J_{01} (A/cm^2)	J_{02} (A/cm^2)
0 %	796.2	74.7	2.07	2.278 E-16	1.687 E-7
11.5 %	882.5	80.1	1.59	2.804 E-16	2.366 E-8
16.0 %	924.1	83.5	1.25	1.247 E-16	5.600 E-9
20.0 %	908.8	74.8	1.91	3.666 E-17	1.743 E-8

Table 3 Capacitance voltage (CV) and drive level capacitance profiling (DLCP)

Sample	X_{dl} (nm)	N_{dl} (cm^{-3})	N_{CV} (cm^{-3})	Carrier Concentration (cm^{-3})
0 %	244.43	5.28 E+15	1.48 E+16	9.51 E+15
11.5 %	359.48	6.80 E+15	1.70 E+16	1.02 E+16
16.0 %	272.20	9.10 E+15	2.16 E+16	1.25 E+16
20.0 %	583.54	1.55 E+15	8.84 E+15	7.29 E+15

To understand the nature of V_{OC} improvement on the devices, we performed Suns – V_{OC} characteristics, as shown in Table 1. The ideality factor reduced from 2.07 to 1.25 and J_{02} decreased from 1.687 E-7 A/cm^2 to 5.600 E-9 A/cm^2 with 16.0 % Ag-alloying, respectively, indicating that Ag-alloying can strength the hetero-junction quality. 0 % to 16.0 % Ag-alloying demonstrated a similar bulk quality with similar J_{01}. As of 20.0 % Ag-alloying, J_{01} decreased one order of magnitude, indicating a better bulk quality with 20.0 % Ag-alloying.
Capacitance voltage and drive level capacitance profiling indicates that the carrier concentration slightly arises from 9.51 E+15 cm^{-3} to 1.25 E+16 cm^{-3}, this can also be considered as one of the reasons for FF gains. From the perspective of EQE, samples with 11.5 % and 16.0 % Ag-alloying outperform the non-Ag alloying sample across the entire wavelength. This is consistent with the increase in J_{SC} despite the bandgap slightly increased from 1.57 eV to 1.59 eV. This further verifies the improvement on hetero-junction interface, which is possibly driven by the reduced recombination enabled by minimizing the CBO.

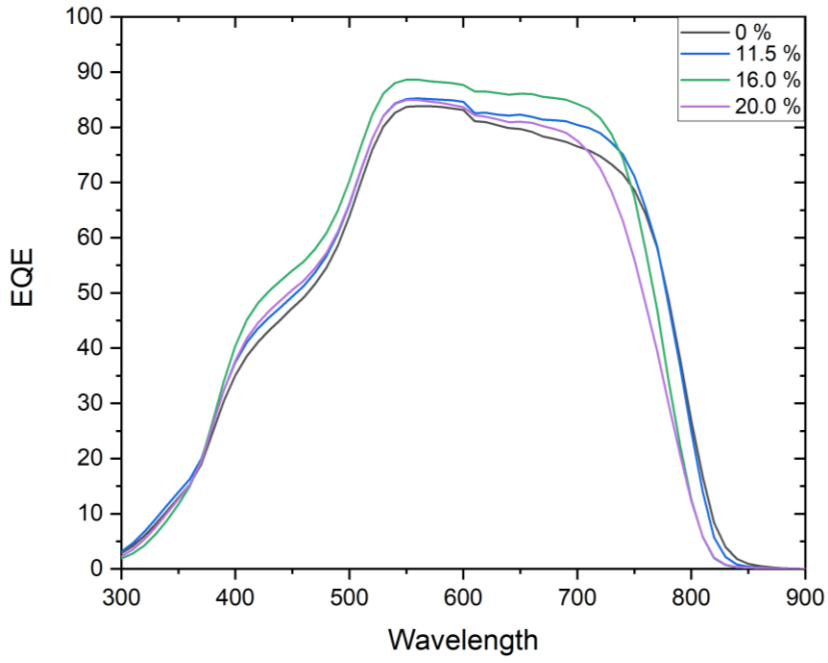

Figure 3. External quantum efficiency (EQE) of different Ag (%)-alloyed CIGS

Conclusion

In this work, we developed a cation substitution enabled by Ag-alloying via sputter method. We carefully investigated the influence of different amount Ag-alloying. SEM and XRD demonstrate that Ag-alloying did not benefit the crystallinity and grain growth, unlike many have reported. The major improvement of Ag-alloying may be driven by the advancement of the hetero-junction interface. Although the interface defect density did not reduce significantly, the gains from the interface might be benefited from the reduction in CBO. In our case, the optimal Ag-alloyed percentage seems to be 16.0 %, which demonstrates 12.24 % efficiency with 887.97 mV V_{OC} without ARC. Future research would be focused on reducing interface recombination by introducing alternative buffer layer and a better sulfurization process to enable a better bulk quality. The goal would be achieving over 1 V V_{OC} CIGS with greater than 15.0 % efficiency, which would be more appropriate as a top cell candidate for tandem solar cells.

References

1. Jost, M.; Kegelmann, L.; Korte, L.; Albrecht, S., Monolithic Perovskite Tandem Solar Cells: A Review of the Present Status and Advanced Characterization Methods Toward 30% Efficiency. *Adv Energy Mater* **2020,** *10* (26).

2. Todorov, T. K.; Bishop, D. M.; Lee, Y. S., Materials perspectives for next-generation low-cost tandem solar cells. *Sol Energ Mat Sol C* **2018,** *180*, 350-357.

3. He, G. J.; Yan, C.; Li, J. J.; Yuan, X. J.; Sun, K. W.; Huang, J. L.; Sun, H.; He, M. R.; Zhang, Y. F.; Stride, J. A.; Green, M. A.; Hao, X. J., 11.6% Efficient Pure Sulfide Cu(In,Ga)S-2 Solar Cell through a Cu-Deficient and KCN-Free Process. *Acs Appl Energ Mater* **2020,** *3* (12), 11974-11980.

4. Green, M. A.; Dunlop, E. D.; Yoshita, M.; Kopidakis, N.; Bothe, K.; Siefer, G.; Hao, X. J., Solar cell efficiency tables (version 62). *Prog Photovoltaics* **2023,** *31* (7), 651-663.

5. Hiroi, H.; Iwata, Y.; Adachi, S.; Sugimoto, H.; Yamada, A., New World-Record Efficiency for Pure-Sulfide Cu(In,Ga)S-2 Thin-Film Solar Cell With Cd-Free Buffer Layer via KCN-Free Process. *Ieee J Photovolt* **2016,** *6* (3), 760-763.

6. Keller, J.; Sopiha, K. V.; Stolt, O.; Stolt, L.; Persson, C.; Scragg, J. J. S.; Torndahl, T.; Edoff, M., Wide-gap (Ag,Cu)(In,Ga)Se-2 solar cells with different buffer materials-A path to a better heterojunction. *Prog Photovoltaics* **2020,** *28* (4), 237-250.

7. Siebentritt, S.; Lomuscio, A.; Adeleye, D.; Sood, M.; Dwivedi, A., Sulfide Chalcopyrite Solar Cells--Are They the Same as Selenides with a Wider Bandgap? *Phys Status Solidi-R* **2022,** *16* (8).